

Study of Z Bosons Produced in Association with Charm in the Forward Region

R. Aaij *et al.*^{*}
(LHCb Collaboration)

(Received 17 September 2021; revised 17 December 2021; accepted 28 January 2022; published 24 February 2022)

Events containing a Z boson and a charm jet are studied for the first time in the forward region of proton-proton collisions. The data sample used corresponds to an integrated luminosity of 6 fb^{-1} collected at a center-of-mass energy of 13 TeV with the LHCb detector. In events with a Z boson and a jet, the fraction of charm jets is determined in intervals of Z -boson rapidity in the range $2.0 < y(Z) < 4.5$. A sizable enhancement is observed in the forwardmost $y(Z)$ interval, which could be indicative of a valencelike intrinsic-charm component in the proton wave function.

DOI: 10.1103/PhysRevLett.128.082001

The possibility that the proton wave function may contain a $|uudc\bar{c}\rangle$ component, referred to as intrinsic charm (IC), in addition to the charm content that arises due to perturbative gluon radiation, i.e., $g \rightarrow c\bar{c}$ splitting, has been debated for decades (for a recent review, see Ref. [1]). The light front QCD calculations of Refs. [2,3], referred to as the Brodsky-Hoyer-Peterson-Sakai (BHPS) model, predict that nonperturbative IC manifests as valencelike charm content in the parton distribution functions (PDFs) of the proton; whereas, if the c -quark content is entirely perturbative in nature, the charm PDF resembles that of the gluon and sharply decreases at large momentum fractions x . (Charge conjugation is implied throughout this Letter, e.g., charm refers to both the c and \bar{c} quarks.) Understanding the role that nonperturbative dynamics play inside the nucleon is a fundamental goal of nuclear physics [4–15]. Furthermore, the existence of IC would have many phenomenological consequences. For example, IC would alter both the rate and kinematics of c hadrons produced by cosmic-ray proton interactions in the atmosphere, which are an important source of background in studies of astrophysical neutrinos [16–21]. The cross sections of many processes at the LHC and other accelerators would also be affected [22–32].

Measurements of c -hadron production in deep inelastic scattering [33] and in fixed-target experiments [34], where the typical momentum transfers were $Q \lesssim 10 \text{ GeV}$ (natural units are used throughout this Letter), have been interpreted both as evidence for [35,36] and against [37] the percent-level IC content predicted by BHPS. Even though such

experiments are in principle sensitive to valencelike c -quark content, interpreting these low- Q data is challenging since it requires careful theoretical treatment of non-perturbative hadronic and nuclear effects. Recent global PDF analyses, which also include measurements from the LHC, are inconclusive and can only exclude IC carrying more than a few percent of the momentum of the proton [38,39].

Reference [29] proposed probing IC by studying events containing a Z boson and a charm jet Zc in the forward region of proton-proton (pp) collisions at the LHC. The ratio of production cross sections $\mathcal{R}_j^c \equiv \sigma(Zc)/\sigma(Zj)$, where Zj refers to events containing a Z boson and any type of jet, was chosen because it is less sensitive than $\sigma(Zc)$ to experimental and theoretical uncertainties. Since Zc production is inherently at large Q , above the electro-weak scale, hadronic effects are small. A leading-order Zc production mechanism is $gc \rightarrow Zc$ scattering (see Fig. 1), where in the forward region one of the initial partons must have large x , hence Zc production probes the valencelike region (Fig. S4 of Supplemental Material shows the x regions probed). Using next-to-leading-order (NLO) standard model (SM) calculations, Fig. 2 illustrates that a percent-level valencelike IC contribution would produce a clear enhancement in \mathcal{R}_j^c for large (more forward) values of Z rapidity, $y(Z)$; whereas only small effects are expected in the central region where all previous measurements of \mathcal{R}_j^c were made [40,41].

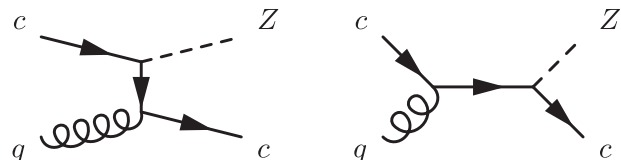


FIG. 1. Leading-order Feynman diagrams for $gc \rightarrow Zc$ production.

*Full author list given at the end of the article.

Published by the American Physical Society under the terms of the Creative Commons Attribution 4.0 International license. Further distribution of this work must maintain attribution to the author(s) and the published article's title, journal citation, and DOI. Funded by SCOAP³.

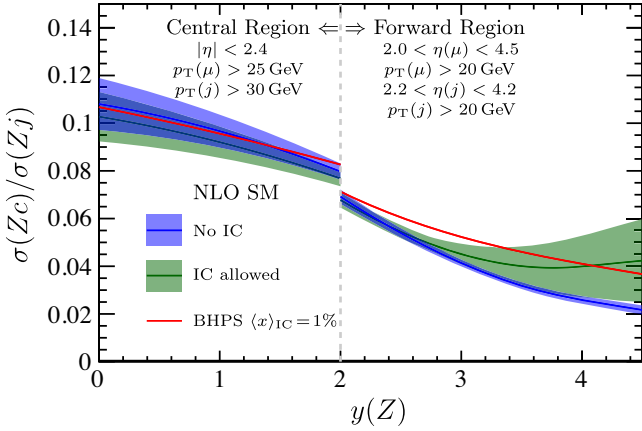


FIG. 2. NLO SM predictions [29] for \mathcal{R}_j^c without IC [42], allowing for potential IC [39], and with the valencelike IC predicted by BHPs with a mean momentum fraction of 1% [38]. The fiducial region from Ref. [41] is used for $y(Z) < 2$; otherwise the fiducial region of this analysis is employed. The broadening of the error band that arises in the forward region, when allowing for IC, is due to the lack of sensitivity to valencelike IC from previous experiments. More details on these calculations are provided in Supplemental Material [43]. The error bands shown for the first two predictions display the 68% confidence-level regions. Only the central value is shown for BHPs due to the charm PDF being fixed.

This Letter presents the first measurement of \mathcal{R}_j^c in the forward region of pp collisions. The data sample used corresponds to an integrated luminosity of 6 fb^{-1} collected at a center-of-mass energy of $\sqrt{s} = 13 \text{ TeV}$ with the LHCb detector. The Z bosons are reconstructed using the $Z \rightarrow \mu^+ \mu^-$ decay, where henceforth all $Z/\gamma^* \rightarrow \mu^+ \mu^-$ production in the mass range $60 < m(\mu^+ \mu^-) < 120 \text{ GeV}$ is labeled $Z \rightarrow \mu^+ \mu^-$. The analysis is performed using jets clustered with the anti- k_T algorithm [44] using a distance parameter $R = 0.5$. The fiducial region is defined in terms of the transverse momentum p_T , pseudorapidity η , and azimuthal angle ϕ of the muon and jet momenta, and includes a requirement on $\Delta R(\mu, j) \equiv \sqrt{\Delta\eta(\mu, j)^2 + \Delta\phi(\mu, j)^2}$ to ensure that the muons and jets are well separated, which suppresses backgrounds from QCD multijet events and electroweak processes like $W + \text{jet}$ production. Charm jets are the subset for which there is a promptly produced and weakly decaying c hadron within the jet. The fiducial region is defined in Table I. If multiple jets satisfy these criteria, the one with the highest p_T is selected. No requirement is placed on the maximum number of jets in the event.

The quantity \mathcal{R}_j^c is measured in intervals of $y(Z)$ as $\mathcal{R}_j^c = N(c\text{-tag})/[\epsilon(c\text{-tag})N(j)]$, where $N(c\text{-tag})$ is the observed Zc yield, $\epsilon(c\text{-tag})$ is the c -tagging efficiency, and $N(j)$ is the total Zj yield. The integrated luminosity does not enter this expression because \mathcal{R}_j^c involves a ratio of production cross sections. In addition, the muon and jet

reconstruction efficiencies largely cancel in the ratio due to the similarity of the Z boson and jet kinematics in Zc and Zj production. The c -tagging algorithm, which is described in detail in Ref. [45], looks for a displaced-vertex (DV) signature inside the jet cone that is indicative of the weak decay of a c hadron.

The LHCb detector is a single-arm forward spectrometer covering the pseudorapidity range $2 < \eta < 5$, described in detail in Refs. [46,47]. Simulated data samples are used to evaluate the detector response for jet reconstruction, including the c -tagging efficiency, and to validate the analysis. In the simulation, pp collisions are generated using PYTHIA [48] with a specific LHCb configuration [49]. Decays of unstable particles are described by EVTGEN [50], in which final-state QED radiation is generated using PHOTOS [51]. The interaction of the generated particles with the detector, and its response, are implemented using the GEANT4 toolkit [52] as described in Ref. [53].

The online event selection is performed by a trigger [54,55] consisting of a hardware stage using information from the calorimeter and muon systems, followed by a software stage that performs a full event reconstruction. At the hardware stage, events are required to have a muon with $p_T(\mu) > 6 \text{ GeV}$. In the software stage, the muon track is required to be of good quality and to have $p_T(\mu) > 10 \text{ GeV}$. The off-line selection builds $Z \rightarrow \mu^+ \mu^-$ candidates from two oppositely charged muon tracks that must be in the fiducial region defined in Table I and consistent with originating directly from the same pp collision.

Jet reconstruction is performed off-line by clustering charged and neutral particle-flow candidates [56] using the anti- k_T clustering algorithm as implemented in FASTJET [57]. Reconstructed jets with $15 < p_T(j) < 100 \text{ GeV}$ and $2.2 < \eta(j) < 4.2$ are kept for further analysis. Jets with $15 < p_T(j) < 20 \text{ GeV}$, which are outside of the fiducial region, are retained for use when unfolding the detector response. The $\eta(j)$ requirement, which is included in the fiducial region and was first used in Refs. [58–60], ensures a nearly uniform c -tagging efficiency of about 24%, with minimal $p_T(j)$ or $\eta(j)$ dependence. The fiducial requirement $\Delta R(\mu, j) > 0.5$ is applied to reconstructed jets. Finally, the highest- p_T jet satisfying these criteria from the same pp collision as the Z boson is selected. After applying all requirements, 68 694 Zj candidates remain in the dataset.

The effects of the detector response on the measured jet momenta are accounted for using an unfolding procedure. This involves first determining the reconstructed Zc and Zj yields in intervals of $[y(Z), p_T(j)]$. The non- Z background is neglected for both Zc and Zj candidates because it is less than 1% and largely cancels in the \mathcal{R}_j^c ratio. The c -jet yields are determined using the DV-based tagging approach described in detail in the following paragraphs. Interval migration is accounted for by unfolding the $p_T(j)$ distributions of the Zc and Zj yields in each $y(Z)$ interval

TABLE I. Definition of the fiducial region.

Z bosons	$p_T(\mu) > 20 \text{ GeV}$, $2.0 < \eta(\mu) < 4.5$, $60 < m(\mu^+ \mu^-) < 120 \text{ GeV}$
Jets	$20 < p_T(j) < 100 \text{ GeV}$, $2.2 < \eta(j) < 4.2$
Charm jets	$p_T(c \text{ hadron}) > 5 \text{ GeV}$, $\Delta R(j, c \text{ hadron}) < 0.5$
Events	$\Delta R(\mu, j) > 0.5$

independently using an iterative Bayesian procedure [61,62]. The Zc yields are then corrected for c -tagging inefficiency. Finally, the unfolded $[y(Z), p_T(j)]$ distributions are integrated for $p_T(j) > 20 \text{ GeV}$ to obtain the Zc and Zj yields used to determine the \mathcal{R}_j^c ratios. The analysis employs three $y(Z)$ intervals with ranges 2.00–2.75, 2.75–3.50, and 3.50–4.50, and four $p_T(j)$ intervals ranging 15–20, 20–30, 30–50, and 50–100 GeV, where after unfolding the yields in the three highest $p_T(j)$ intervals are summed to obtain \mathcal{R}_j^c .

The signature of a c jet is the presence of a long-lived c hadron that carries a sizable fraction of the jet energy. The tagging of c jets is performed using DVs formed from the decays of such c hadrons. The choice of using DVs and not single-track or other non-DV-based jet properties, e.g., the number of particles in the jet, is driven by the need for a small misidentification probability of light-parton jets. Furthermore, the properties of DVs from c -hadron decays are known to be well modeled by simulation, which means that only small corrections using control samples are required. Since DVs can also be formed from the decays of b hadrons or due to artifacts of the reconstruction, the DV-tagged charm yields are obtained by fitting the distributions of DV features with good discrimination power between c , b , and light-parton jets.

The tracks used as inputs to the DV-tagger algorithm are required to have $p_T > 0.5 \text{ GeV}$ and to be inconsistent with originating directly from a pp interaction point. A DV is associated to a jet when $\Delta R < 0.5$ between the jet axis and the DV direction of flight, defined by the vector from the pp interaction point to the DV position. Requirements that reject strange-hadron decays and particles formed in

interactions with material [63] are placed on the mass, $m(\text{DV})$, and momentum, $p(\text{DV})$, of the particles that form the DV, along with the DV position. In addition, only DVs with at most four tracks are used, since higher-multiplicity DVs are almost exclusively due to b -hadron decays. More details about the c -tagging algorithm are provided in Ref. [45].

Two DV properties are used to separate charm jets from beauty and light-parton jets: the number of tracks in the DV, $N_{\text{trk}}(\text{DV})$, and the corrected mass, $m_{\text{cor}}(\text{DV}) \equiv \sqrt{m(\text{DV})^2 + [p(\text{DV}) \sin \theta]^2} + p(\text{DV}) \sin \theta$, where θ is the angle between the momentum and the flight direction of the DV. The corrected mass, which is the minimum mass the long-lived hadron can have that is consistent with the flight direction, peaks near the typical c -hadron mass for c jets, and consequently provides excellent discrimination against other jet types. The DV track multiplicity provides additional discrimination against b jets, since b -hadron decays often produce many displaced tracks. These two distributions are fitted simultaneously to obtain the DV-tagged c -jet yields. The probability density functions, referred to as templates, for c , b , and light-parton jets are obtained from calibration data samples that are each highly enriched in a given jet flavor [45]. Figure 3 shows the $m_{\text{cor}}(\text{DV})$ and $N_{\text{trk}}(\text{DV})$ distributions for all DV-tagged candidates in the Zj data sample reconstructed in the fiducial region, along with the fit projections; such fits are performed in each $[y(Z), p_T(j)]$ interval to obtain the reconstructed Zc yields.

The effects of $p_T(j)$ interval migration are corrected for using the unfolding procedure. The detector response is studied using the p_T -balance distribution $p_T(j)/p_T(Z)$ for Zj candidates that are nearly back-to-back in the transverse plane, using the same technique as in Refs. [56,64]. Small adjustments are applied to the $p_T(j)$ scale and resolution in simulation to obtain the best agreement with data. In addition, for the Zc and Zj samples the $p_T(j)$ and $p_T(\text{DV})$ distributions in simulation are adjusted to match those observed in data. The unfolding matrix for jets that contain a reconstructed DV is shown in Fig. 4, while the corresponding matrix for inclusive Zj production is provided in Supplemental Material [43].

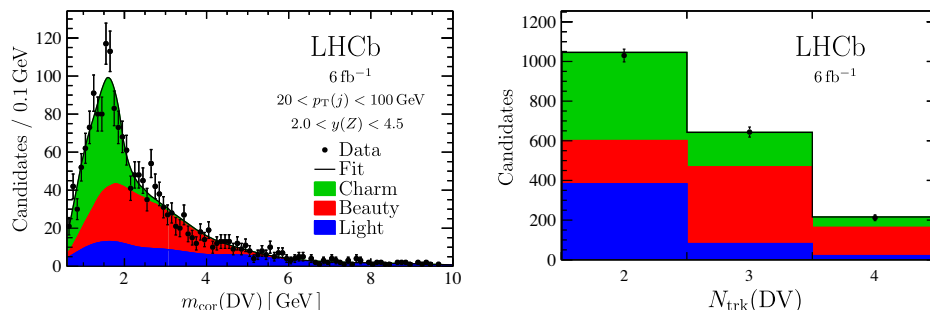


FIG. 3. Distributions of (left) $m_{\text{cor}}(\text{DV})$ and (right) $N_{\text{trk}}(\text{DV})$ for all DV-tagged candidates in the Zj data sample reconstructed in the fiducial region with the projections of the fit results superimposed.

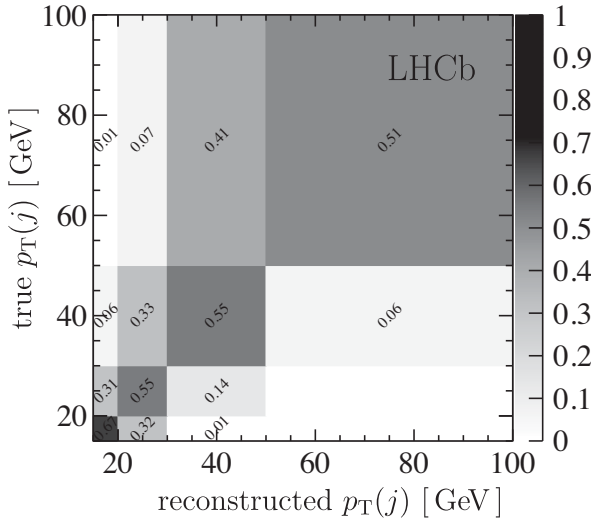


FIG. 4. The detector-response matrix for c -tagged jets. The shading represents the interval-to-interval migration probabilities ranging from (white) 0 to (black) 1. Numerical labels are only shown for values greater than 1%. Jets with true (reconstructed) $p_T(j)$ in the 20–100 GeV region but for which the reconstructed (true) $p_T(j)$ is either below 15 GeV or above 100 GeV are included in the unfolding but not shown graphically.

The dominant systematic uncertainty is due to limited knowledge of the c -tagging efficiency, which is measured in $p_T(j)$ intervals using data in Ref. [45] and briefly summarized here. Scale factors that correct for discrepancies between data and simulation are determined using a tag-and-probe approach on a dijet calibration sample. A stringent requirement is applied to the tag jet which enriches the probe-jet sample in charm content. The DV-tagged c -jet yield in the probe sample is obtained in the same way the Zc yield is determined in this analysis, namely by fitting the $m_{\text{cor}}(\text{DV})$ and $N_{\text{trk}}(\text{DV})$ distributions for DV-tagged probe jets. The total number of c jets in the probe sample is obtained by fully reconstructing the $D^0 \rightarrow K^-\pi^+$ and $D^+ \rightarrow K^-\pi^+\pi^+$ decays, obtaining the prompt-charm yields by fitting the D -meson mass and impact-parameter distributions, then correcting these yields for the detector response, decay branching fractions [65], and c -hadron fragmentation fractions [66]. The c -tagging efficiency is the ratio of the DV-tagged and total c -jet probe-sample yields. The scale factors that correct the c -tagging efficiency in simulation are determined to be 1.03 ± 0.06 , 1.01 ± 0.08 , and 1.09 ± 0.17 in the 20–30, 30–50, and 50–100 GeV $p_T(j)$ intervals, respectively, with corresponding c -tagging efficiencies of $(23.9 \pm 1.4)\%$, $(24.4 \pm 1.9)\%$, and $(23.6 \pm 4.1)\%$. These uncertainties, which include all statistical and systematic contributions, are propagated to the \mathcal{R}_j^c results producing 6%–7% relative uncertainties in each $y(Z)$ interval.

Other sources of smaller systematic uncertainty are also considered. First, variations of the $m_{\text{cor}}(\text{DV})$ and $N_{\text{trk}}(\text{DV})$

TABLE II. Relative systematic uncertainties on \mathcal{R}_j^c , where ranges indicate that the value depends on the $y(Z)$ intervals.

Source	Relative uncertainty
c tagging	6%–7%
DV-fit templates	3%–4%
Jet reconstruction	1%
Jet p_T scale and resolution	1%
Total	8%

templates are studied, which arise from using different strategies to model the backgrounds in the highly enriched calibration data samples. However, the shifts observed in the Zc yields largely cancel with the corresponding shifts seen in $\epsilon(c\text{-tag})$. The residual differences of 3%–4% in each $y(Z)$ interval are assigned as systematic uncertainties. The ratio of the jet-reconstruction efficiency for c and inclusive jets is consistent with unity in all kinematic intervals in simulation, with a 1% systematic uncertainty assigned due to the limited sample sizes. Finally, the statistical precision of the back-to-back Zj sample used to determine the $p_T(j)$ scale and resolution is propagated through the unfolding procedure resulting in a 1% relative systematic uncertainty on \mathcal{R}_j^c . The systematic uncertainties are summarized in Table II.

Figure 5 shows the measured \mathcal{R}_j^c distribution in intervals of $y(Z)$; the numerical results are provided in Table III, and additional results are reported in Supplemental Material [43]. The measured \mathcal{R}_j^c values are compared to NLO SM calculations [29] based on Refs. [67–73], which are validated against additional predictions [70,71,74,75] and updated here to use more recent PDFs [38,39,42,76,77].

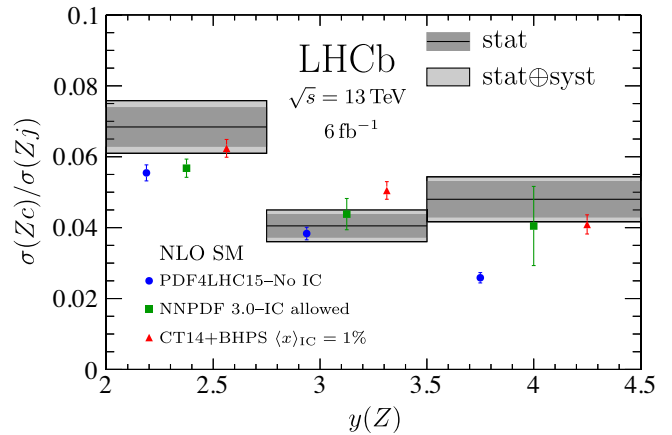


FIG. 5. Measured \mathcal{R}_j^c distribution (gray bands) for three intervals of forward Z rapidity, compared to NLO SM predictions [29] without IC [42], with the charm PDF shape allowed to vary (hence, permitting IC) [39,76], and with IC as predicted by BHPS with a mean momentum fraction of 1% [38]. The predictions are offset in each interval to improve visibility.

TABLE III. Numerical results for the \mathcal{R}_j^c measurements, where the first uncertainty is statistical and the second is systematic.

$y(Z)$	\mathcal{R}_j^c (%)
2.00–2.75	$6.84 \pm 0.54 \pm 0.51$
2.75–3.50	$4.05 \pm 0.32 \pm 0.31$
3.50–4.50	$4.80 \pm 0.50 \pm 0.39$
2.00–4.50	$4.98 \pm 0.25 \pm 0.35$

While Zc predictions at next-to-next-to-leading-order in QCD are not available, Zb predictions are [78], and similar methods should be applicable. The NNPDF Collaboration analysis provides results where the charm PDF is allowed to vary, both in size and in shape [39]. The sizable uncertainties that arise in the forward region are due to the lack of sensitivity to valencelike IC from previous experiments. Reference [38] updated the CT14 analysis [79] to include the IC content predicted by BHPS [2,3], which results in the enhancement at forward $y(Z)$ shown previously in Fig. 2. These predictions have smaller uncertainties because the size and shape of the IC contribution are fixed, i.e., the IC contribution is assumed to be known, hence does not contribute to the uncertainty on \mathcal{R}_j^c . More details on the theory calculations, along with predictions based on other PDFs [80–82], are provided in Supplemental Material [43].

The observed \mathcal{R}_j^c values are consistent with both the no-IC and IC hypotheses in the first two $y(Z)$ intervals; however, this is not the case in the forwardmost interval where the ratio of the observed to no-IC-expected values is 1.85 ± 0.25 . As illustrated in Fig. 2, this is precisely the $y(Z)$ region where valencelike IC would cause a large enhancement. Indeed, Fig. 5 shows that, after including the IC PDF shape predicted by BHPS with a mean momentum fraction of 1%, the theory predictions are consistent with the data. Incorporating these novel forward \mathcal{R}_j^c results into a global analysis should strongly constrain the large- x charm PDF, both in size and in shape. While the large enhancement in the forwardmost $y(Z)$ interval is suggestive of valencelike IC, no definitive statements can be made until the \mathcal{R}_j^c results are included in a global PDF analysis.

In conclusion, events containing a Z boson and a charm jet are studied for the first time in the forward region of pp collisions. The data sample used corresponds to an integrated luminosity of 6 fb^{-1} collected at a center-of-mass energy of 13 TeV with the LHCb detector. The ratio \mathcal{R}_j^c is measured in intervals of $y(Z)$ and compared to NLO SM calculations. The observed spectrum exhibits a sizable enhancement at forward Z rapidities, consistent with the effect expected if the proton wave function contains the $|uudc\bar{c}\rangle$ component predicted by BHPS. However, conclusions about whether the proton contains valencelike

intrinsic charm can only be drawn after incorporating these results into global PDF analyses.

We express our gratitude to our colleagues in the CERN accelerator departments for the excellent performance of the LHC. We thank the technical and administrative staff at the LHCb institutes. We acknowledge support from CERN and from the national agencies: CAPES, CNPq, FAPERJ, and FINEP (Brazil); MOST and NSFC (China); CNRS/IN2P3 (France); BMBF, DFG, and MPG (Germany); INFN (Italy); NWO (Netherlands); MNiSW and NCN (Poland); MEN/IFA (Romania); MSHE (Russia); MICINN (Spain); SNSF and SER (Switzerland); NASU (Ukraine); STFC (United Kingdom); DOE NP and NSF (USA). We acknowledge the computing resources that are provided by CERN, IN2P3 (France), KIT and DESY (Germany), INFN (Italy), SURF (Netherlands), PIC (Spain), GridPP (United Kingdom), RRCKI and Yandex LLC (Russia), CSCS (Switzerland), IFIN-HH (Romania), CBPF (Brazil), PL-GRID (Poland), and NERSC (USA). We are indebted to the communities behind the multiple open-source software packages on which we depend. Individual groups or members have received support from ARC and ARDC (Australia); AvH Foundation (Germany); EPLANET, Marie Skłodowska-Curie Actions and ERC (European Union); A*MIDEX, ANR, IPhU and Labex P2IO, and Région Auvergne-Rhône-Alpes (France); Key Research Program of Frontier Sciences of CAS, CAS PIFI, CAS CCEPP, Fundamental Research Funds for the Central Universities, and Sci. & Tech. Program of Guangzhou (China); RFBR, RSF, and Yandex LLC (Russia); GVA, XuntaGal, and GENCAT (Spain); the Leverhulme Trust, the Royal Society, and UKRI (United Kingdom).

- [1] S. J. Brodsky, A. Kusina, F. Lyonnet, I. Schienbein, H. Spiesberger, and R. Vogt, A review of the intrinsic heavy quark content of the nucleon, *Adv. High Energy Phys.* **2015**, 231547 (2015).
- [2] S. J. Brodsky, P. Hoyer, C. Peterson, and N. Sakai, The intrinsic charm of the proton, *Phys. Lett.* **93B**, 451 (1980).
- [3] S. J. Brodsky, C. Peterson, and N. Sakai, Intrinsic heavy quark states, *Phys. Rev. D* **23**, 2745 (1981).
- [4] E. Hoffmann and R. Moore, Subleading contributions to the intrinsic charm of the nucleon, *Z. Phys. C* **20**, 71 (1983).
- [5] F. S. Navarra, M. Nielsen, C. A. A. Nunes, and M. Teixeira, On the intrinsic charm component of the nucleon, *Phys. Rev. D* **54**, 842 (1996).
- [6] M. Franz, M. V. Polyakov, and K. Goeke, Heavy quark mass expansion and intrinsic charm in light hadrons, *Phys. Rev. D* **62**, 074024 (2000).
- [7] J. Pumplin, Light-cone models for intrinsic charm and bottom, *Phys. Rev. D* **73**, 114015 (2006).
- [8] W. Freeman and D. Toussaint (MILC Collaboration), Intrinsic strangeness and charm of the nucleon using improved staggered fermions, *Phys. Rev. D* **88**, 054503 (2013).

- [9] S. Brodsky, G. de Teramond, and M. Karliner, Puzzles in hadronic physics and novel quantum chromodynamics phenomenology, *Annu. Rev. Nucl. Part. Sci.* **62**, 1 (2012).
- [10] M. Gong, A. Alexandru, Y. Chen, T. Doi, S. J. Dong, T. Draper, W. Freeman, M. Glatzmaier, A. Li, K. F. Liu, and Z. Liu (XQCD Collaboration), Strangeness and charmness content of the nucleon from overlap fermions on 2 + 1-flavor domain-wall fermion configurations, *Phys. Rev. D* **88**, 014503 (2013).
- [11] T. J. Hobbs, J. T. Londergan, and W. Melnitchouk, Phenomenology of nonperturbative charm in the nucleon, *Phys. Rev. D* **89**, 074008 (2014).
- [12] R. D. Ball, V. Bertone, M. Bonvini, S. Forte, P. G. Merrild, J. Rojo, and L. Rottoli, Intrinsic charm in a matched general-mass scheme, *Phys. Lett. B* **754**, 49 (2016).
- [13] J. Blümlein, A kinematic condition on intrinsic charm, *Phys. Lett. B* **753**, 619 (2016).
- [14] S. Duan, C. S. An, and B. Saghai, Intrinsic charm content of the nucleon and charmness-nucleon sigma term, *Phys. Rev. D* **93**, 114006 (2016).
- [15] R. S. Sufian, T. Liu, A. Alexandru, S. J. Brodsky, G. F. de Téramond, H. G. Dosch, T. Draper, K.-F. Liu, and Y.-B. Yang, Constraints on charm-anticharm asymmetry in the nucleon from lattice QCD, *Phys. Lett. B* **808**, 135633 (2020).
- [16] M. G. Aartsen *et al.* (IceCube Collaboration), Evidence for high-energy extraterrestrial neutrinos at the IceCube detector, *Science* **342**, 1242856 (2013).
- [17] R. Gauld, J. Rojo, L. Rottoli, S. Sarkar, and J. Talbert, The prompt atmospheric neutrino flux in the light of LHCb, *J. High Energy Phys.* **02** (2016) 130.
- [18] F. Halzen and L. Wille, Charm contribution to the atmospheric neutrino flux, *Phys. Rev. D* **94**, 014014 (2016).
- [19] R. Laha and S. J. Brodsky, IceCube can constrain the intrinsic charm of the proton, *Phys. Rev. D* **96**, 123002 (2017).
- [20] A. V. Giannini, V. P. Gonçalves, and F. S. Navarra, Intrinsic charm contribution to the prompt atmospheric neutrino flux, *Phys. Rev. D* **98**, 014012 (2018).
- [21] V. P. Goncalves, R. Maciula, and A. Szczurek, Impact of intrinsic charm amount in the nucleon and saturation effects on the prompt atmospheric ν_μ flux for IceCube, [arXiv: 2103.05503](https://arxiv.org/abs/2103.05503).
- [22] H. L. Lai, P. Nadolsky, J. Pumplin, D. Stump, W.-K. Tung, and C.-P. Yuan, The Strange parton distribution of the nucleon: Global analysis and applications, *J. High Energy Phys.* **04** (2007) 089.
- [23] S. J. Brodsky, A. S. Goldhaber, B. Z. Kopeliovich, and I. Schmidt, Higgs hadroproduction at large Feynman x , *Nucl. Phys.* **B807**, 334 (2009).
- [24] T. P. Stavreva and J. F. Owens, Direct photon production in association with a heavy quark at hadron colliders, *Phys. Rev. D* **79**, 054017 (2009).
- [25] V. A. Bednyakov, M. A. Demichev, G. I. Lykasov, T. Stavreva, and M. Stockton, Searching for intrinsic charm in the proton at the LHC, *Phys. Lett. B* **728**, 602 (2014).
- [26] S. Dulat, T. J. Hou, J. Gao, J. Huston, J. Pumplin, C. Schmidt, D. Stump, and C. P. Yuan, Intrinsic charm parton distribution functions from CTEQ-TEA global analysis, *Phys. Rev. D* **89**, 073004 (2014).
- [27] F. Halzen, Y. S. Jeong, and C. S. Kim, Charge asymmetry of weak boson production at the LHC and the charm content of the proton, *Phys. Rev. D* **88**, 073013 (2013).
- [28] S. Rostami, A. Khorramian, A. Aleedaneshvar, and M. Goharipour, The impact of the intrinsic charm quark content of a proton on the differential $\gamma + c$ cross section, *J. Phys. G* **43**, 055001 (2016).
- [29] T. Boettcher, P. Ilten, and M. Williams, Direct probe of the intrinsic charm content of the proton, *Phys. Rev. D* **93**, 074008 (2016).
- [30] G. Bailas and V. P. Goncalves, Phenomenological implications of the intrinsic charm in the Z boson production at the LHC, *Eur. Phys. J. C* **76**, 105 (2016).
- [31] A. V. Lipatov, G. I. Lykasov, Y. Y. Stepanenko, and V. A. Bednyakov, Probing proton intrinsic charm in photon or Z boson production accompanied by heavy jets at the LHC, *Phys. Rev. D* **94**, 053011 (2016).
- [32] W. Bai and M. H. Reno, Prompt neutrinos and intrinsic charm at SHiP, *J. High Energy Phys.* **02** (2019) 077.
- [33] J. J. Aubert *et al.* (European Muon Collaboration), Production of charmed particles in 250-GeV μ^+ -iron interactions, *Nucl. Phys.* **B213**, 31 (1983).
- [34] R. Aaij *et al.* (LHCb Collaboration), First Measurement of Charm Production in Fixed-Target Configuration at the LHC, *Phys. Rev. Lett.* **122**, 132002 (2019).
- [35] B. W. Harris, J. Smith, and R. Vogt, Reanalysis of the EMC charm production data with extrinsic and intrinsic charm at NLO, *Nucl. Phys.* **B461**, 181 (1996).
- [36] F. M. Steffens, W. Melnitchouk, and A. W. Thomas, Charm in the nucleon, *Eur. Phys. J. C* **11**, 673 (1999).
- [37] P. Jimenez-Delgado, T. J. Hobbs, J. T. Londergan, and W. Melnitchouk, New Limits on Intrinsic Charm in the Nucleon from Global Analysis of Parton Distributions, *Phys. Rev. Lett.* **114**, 082002 (2015).
- [38] T.-J. Hou, S. Dulat, J. Gao, M. Guzzi, J. Huston, P. Nadolsky, C. Schmidt, J. Winter, K. Xie, and C.-P. Yuan, CT14 intrinsic charm parton distribution functions from CTEQ-TEA global analysis, *J. High Energy Phys.* **02** (2018) 059.
- [39] R. D. Ball, V. Bertone, M. Bonvini, S. Carrazza, S. Forte, A. Guffanti, N. P. Hartland, J. Rojo, and L. Rottoli (NNPDF Collaboration), A determination of the charm content of the proton, *Eur. Phys. J. C* **76**, 647 (2016).
- [40] V. M. Abazov *et al.* (D0 Collaboration), Measurement of Associated Production of Z Bosons with Charm Quark Jets in $p\bar{p}$ Collisions at $\sqrt{s} = 1.96$ TeV, *Phys. Rev. Lett.* **112**, 042001 (2014).
- [41] A. M. Sirunyan *et al.* (CMS Collaboration), Measurement of the associated production of a Z boson with charm or bottom quark jets in proton-proton collisions at $\sqrt{s} = 13$ TeV, *Phys. Rev. D* **102**, 032007 (2020).
- [42] J. Butterworth *et al.*, PDF4LHC recommendations for LHC Run II, *J. Phys. G* **43**, 023001 (2016).
- [43] See Supplemental Material at <http://link.aps.org-supplemental/10.1103/PhysRevLett.128.082001> for details on the theoretical predictions, and for additional plots and numerical results.
- [44] M. Cacciari, G. P. Salam, and G. Soyez, The anti- k_T jet clustering algorithm, *J. High Energy Phys.* **04** (2008) 063.
- [45] R. Aaij *et al.* (LHCb Collaboration), Identification of charm jets at LHCb, [arXiv:2112.08435](https://arxiv.org/abs/2112.08435).

- [46] A. A. Alves Jr. *et al.* (LHCb Collaboration), The LHCb detector at the LHC, *J. Instrum.* **3**, S08005 (2008).
- [47] R. Aaij *et al.* (LHCb Collaboration), LHCb detector performance, *Int. J. Mod. Phys. A* **30**, 1530022 (2015).
- [48] T. Sjöstrand, S. Mrenna, and P. Skands, A brief introduction to PYTHIA8.1, *Comput. Phys. Commun.* **178**, 852 (2008); T. Sjöstrand, S. Mrenna, and P. Skands, PYTHIA6.4 physics and manual, *J. High Energy Phys.* **05** (2006) 026.
- [49] I. Belyaev *et al.*, Handling of the generation of primary events in Gauss, the LHCb simulation framework, *J. Phys. Conf. Ser.* **331**, 032047 (2011).
- [50] D. J. Lange, The EvtGen particle decay simulation package, *Nucl. Instrum. Methods Phys. Res., Sect. A* **462**, 152 (2001).
- [51] N. Davidson, T. Przedzinski, and Z. Was, PHOTOS interface in C++: Technical and physics documentation, *Comput. Phys. Commun.* **199**, 86 (2016).
- [52] J. Allison *et al.* (Geant4 Collaboration), GEANT4 developments and applications, *IEEE Trans. Nucl. Sci.* **53**, 270 (2006); S. Agostinelli *et al.* (Geant4 Collaboration), GEANT4: A simulation toolkit, *Nucl. Instrum. Methods Phys. Res., Sect. A* **506**, 250 (2003).
- [53] M. Clemencic, G. Corti, S. Easo, C. R. Jones, S. Miglioranzi, M. Pappagallo, and P. Robbe, The LHCb simulation application, Gauss: Design, evolution and experience, *J. Phys. Conf. Ser.* **331**, 032023 (2011).
- [54] R. Aaij *et al.*, The LHCb trigger and its performance in 2011, *J. Instrum.* **8**, P04022 (2013).
- [55] R. Aaij *et al.*, Performance of the LHCb trigger and full real-time reconstruction in Run 2 of the LHC, *J. Instrum.* **14**, P04013 (2019).
- [56] R. Aaij *et al.* (LHCb Collaboration), Study of forward $Z +$ jet production in $p + p$ collisions at $\sqrt{s} = 7$ TeV, *J. High Energy Phys.* **01** (2014) 033.
- [57] M. Cacciari, G. P. Salam, and G. Soyez, FastJet user manual, *Eur. Phys. J. C* **72**, 1896 (2012).
- [58] R. Aaij *et al.* (LHCb Collaboration), Identification of beauty and charm quark jets at LHCb, *J. Instrum.* **10**, P06013 (2015).
- [59] R. Aaij *et al.* (LHCb Collaboration), First Observation of Top Quark Production in the Forward Region, *Phys. Rev. Lett.* **115**, 112001 (2015).
- [60] R. Aaij *et al.* (LHCb Collaboration), Study of W boson production in association with beauty and charm, *Phys. Rev. D* **92**, 052012 (2015).
- [61] G. D'Agostini, A multidimensional unfolding method based on Bayes' theorem, *Nucl. Instrum. Methods Phys. Res., Sect. A* **362**, 487 (1995).
- [62] T. Adye, Unfolding algorithms and tests using RooUnfold, in *Proceedings of the PHYSTAT 2011* (CERN, Geneva, 2011), pp. 313–318.
- [63] M. Alexander *et al.*, Mapping the material in the LHCb vertex locator using secondary hadronic interactions, *J. Instrum.* **13**, P06008 (2018).
- [64] R. Aaij *et al.* (LHCb Collaboration), Study of J/ψ Production in Jets, *Phys. Rev. Lett.* **118**, 192001 (2017).
- [65] P. A. Zyla *et al.* (Particle Data Group), Review of particle physics, *Prog. Theor. Exp. Phys.* **2020**, 083C01 (2020).
- [66] M. Lisovyi, A. Verbytskyi, and O. Zenaiev, Combined analysis of charm-quark fragmentation-fraction measurements, *Eur. Phys. J. C* **76**, 397 (2016).
- [67] S. Alioli, P. Nason, C. Oleari, and E. Re, Vector boson plus one jet production in POWHEG, *J. High Energy Phys.* **01** (2011) 095.
- [68] T. Sjöstrand, S. Ask, J. R. Christiansen, R. Corke, N. Desai, P. Ilten, S. Mrenna, S. Prestel, C. O. Rasmussen, and P. Z. Skands, An introduction to PYTHIA8.2, *Comput. Phys. Commun.* **191**, 159 (2015).
- [69] P. Nason, A new method for combining NLO QCD with shower Monte Carlo algorithms, *J. High Energy Phys.* **11** (2004) 040.
- [70] J. Alwall, R. Frederix, S. Frixione, V. Hirschi, F. Maltoni, O. Mattelaer, H.-S. Shao, T. Stelzer, P. Torrielli, and M. Zaro, The automated computation of tree-level and next-to-leading order differential cross sections, and their matching to parton shower simulations, *J. High Energy Phys.* **07** (2014) 079.
- [71] R. Frederix and S. Frixione, Merging meets matching in MC@NLO, *J. High Energy Phys.* **12** (2012) 061.
- [72] P. Golonka and Z. Was, PHOTOS Monte Carlo: A precision tool for QED corrections in Z and W decays, *Eur. Phys. J. C* **45**, 97 (2006).
- [73] W. T. Giele and S. Keller, Implications of hadron collider observables on parton distribution function uncertainties, *Phys. Rev. D* **58**, 094023 (1998).
- [74] J. M. Campbell, R. K. Ellis, and C. Williams, Vector boson pair production at the LHC, *J. High Energy Phys.* **07** (2011) 018.
- [75] J. M. Campbell, R. K. Ellis, and W. T. Giele, A multi-threaded version of MCFM, *Eur. Phys. J. C* **75**, 246 (2015).
- [76] R. D. Ball, V. Bertone, S. Carrazza, C. S. Deans, L. D. Debbio, S. Forte, A. Guffanti, N. P. Hartland, J. I. Latorre, J. Rojo, and M. Ubiali (NNPDF Collaboration), Parton distributions for the LHC Run II, *J. High Energy Phys.* **04** (2015) 040.
- [77] L. A. Harland-Lang, A. D. Martin, P. Motylinski, and R. S. Thorne, Parton distributions in the LHC era: MMHT 2014 PDFs, *Eur. Phys. J. C* **75**, 204 (2015).
- [78] R. Gauld, A. G. Ridder, E. W. N. Glover, A. Huss, and I. Majer, Predictions for Z -Boson Production in Association with a b -Jet at $\mathcal{O}(\alpha_s^3)$, *Phys. Rev. Lett.* **125**, 222002 (2020).
- [79] S. Dulat, T.-J. Hou, J. Gao, M. Guzzi, J. Huston, P. Nadolsky, J. Pumplin, C. Schmidt, D. Stump, and C.-P. Yuan, New parton distribution functions from a global analysis of quantum chromodynamics, *Phys. Rev. D* **93**, 033006 (2016).
- [80] S. Alekhin, J. Blümlein, and S. Moch, NLO PDFs from the ABMP16 fit, *Eur. Phys. J. C* **78**, 477 (2018).
- [81] P. Jimenez-Delgado and E. Reya, Delineating parton distributions and the strong coupling, *Phys. Rev. D* **89**, 074049 (2014).
- [82] H. Abramowicz *et al.* (H1, ZEUS Collaborations), Combination of measurements of inclusive deep inelastic $e^\pm p$ scattering cross sections and QCD analysis of HERA data, *Eur. Phys. J. C* **75**, 580 (2015).

- R. Aaij,³² A. S. W. Abdelmotteeb,⁵⁶ C. Abellán Beteta,⁵⁰ F. J. Abudinen Gallego,⁵⁶ T. Ackernley,⁶⁰ B. Adeva,⁴⁶ M. Adinolfi,⁵⁴ H. Afsharnia,⁹ C. Agapopoulou,¹³ C. A. Aidala,⁸⁷ S. Aiola,²⁵ Z. Ajaltouni,⁹ S. Akar,⁶⁵ J. Albrecht,¹⁵ F. Alessio,⁴⁸ M. Alexander,⁵⁹ A. Alfonso Albero,⁴⁵ Z. Aliouche,⁶² G. Alkhazov,³⁸ P. Alvarez Cartelle,⁵⁵ S. Amato,² J. L. Amey,⁵⁴ Y. Amhis,¹¹ L. An,⁴⁸ L. Anderlini,²² A. Andreianov,³⁸ M. Andreotti,²¹ F. Archilli,¹⁷ A. Artamonov,⁴⁴ M. Artuso,⁶⁸ K. Arzimatov,⁴² E. Aslanides,¹⁰ M. Atzeni,⁵⁰ B. Audurier,¹² S. Bachmann,¹⁷ M. Bachmayer,⁴⁹ J. J. Back,⁵⁶ P. Baladron Rodriguez,⁴⁶ V. Balagura,¹² W. Baldini,²¹ J. Baptista Leite,¹ M. Barbetti,²² R. J. Barlow,⁶² S. Barsuk,¹¹ W. Barter,⁶¹ M. Bartolini,^{24,b} F. Baryshnikov,⁸³ J. M. Basels,¹⁴ S. Bashir,³⁴ G. Bassi,²⁹ B. Batsukh,⁶⁸ A. Battig,¹⁵ A. Bay,⁴⁹ A. Beck,⁵⁶ M. Becker,¹⁵ F. Bedeschi,²⁹ I. Bediaga,¹ A. Beiter,⁶⁸ V. Belavin,⁴² S. Belin,²⁷ V. Bellee,⁵⁰ K. Belous,⁴⁴ I. Belov,⁴⁰ I. Belyaev,⁴¹ G. Bencivenni,²³ E. Ben-Haim,¹³ A. Berezhnoy,⁴⁰ R. Bernet,⁵⁰ D. Berninghoff,¹⁷ H. C. Bernstein,⁶⁸ C. Bertella,⁴⁸ A. Bertolin,²⁸ C. Betancourt,⁵⁰ F. Betti,⁴⁸ Ia. Bezshyiko,⁵⁰ S. Bhasin,⁵⁴ J. Bhom,³⁵ L. Bian,⁷³ M. S. Bieker,¹⁵ S. Bifani,⁵³ P. Billoir,¹³ M. Birch,⁶¹ F. C. R. Bishop,⁵⁵ A. Bitadze,⁶² A. Bizzeti,^{22,c} M. Bjørn,⁶³ M. P. Blago,⁴⁸ T. Blake,⁵⁶ F. Blanc,⁴⁹ S. Blusk,⁶⁸ D. Bobulska,⁵⁹ J. A. Boelhauve,¹⁵ O. Boente Garcia,⁴⁶ T. Boettcher,⁶⁵ A. Boldyrev,⁸² A. Bondar,⁴³ N. Bondar,^{38,48} S. Borghi,⁶² M. Borisjak,⁴² M. Borsato,¹⁷ J. T. Borsuk,³⁵ S. A. Bouchiba,⁴⁹ T. J. V. Bowcock,⁶⁰ A. Boyer,⁴⁸ C. Bozzi,²¹ M. J. Bradley,⁶¹ S. Braun,⁶⁶ A. Brea Rodriguez,⁴⁶ J. Brodzicka,³⁵ A. Brossa Gonzalo,⁵⁶ D. Brundu,²⁷ A. Buonaura,⁵⁰ L. Buonincontri,²⁸ A. T. Burke,⁶² C. Burr,⁴⁸ A. Bursche,⁷² A. Butkevich,³⁹ J. S. Butter,³² J. Buytaert,⁴⁸ W. Byczynski,⁴⁸ S. Cadeddu,²⁷ H. Cai,⁷³ R. Calabrese,^{21,d} L. Calefice,^{15,13} L. Calero Diaz,²³ S. Cali,²³ R. Calladine,⁵³ M. Calvi,^{26,e} M. Calvo Gomez,⁸⁵ P. Camargo Magalhaes,⁵⁴ P. Campana,²³ A. F. Campoverde Quezada,⁶ S. Capelli,^{26,e} L. Capriotti,^{20,f} A. Carbone,^{20,f} G. Carboni,³¹ R. Cardinale,^{24,b} A. Cardini,²⁷ I. Carli,⁴ P. Carniti,^{26,e} L. Carus,¹⁴ K. Carvalho Akiba,³² A. Casais Vidal,⁴⁶ G. Casse,⁶⁰ M. Cattaneo,⁴⁸ G. Cavallero,⁴⁸ S. Celani,⁴⁹ J. Cerasoli,¹⁰ D. Cervenkov,⁶³ A. J. Chadwick,⁶⁰ M. G. Chapman,⁵⁴ M. Charles,¹³ Ph. Charpentier,⁴⁸ G. Chatzikostantinidis,⁵³ C. A. Chavez Barajas,⁶⁰ M. Chefdeville,⁸ C. Chen,³ S. Chen,⁴ A. Chernov,³⁵ V. Chobanova,⁴⁶ S. Cholak,⁴⁹ M. Chrzaszcz,³⁵ A. Chubykin,³⁸ V. Chulikov,³⁸ P. Ciambrone,²³ M. F. Cicala,⁵⁶ X. Cid Vidal,⁴⁶ G. Ciezarek,⁴⁸ P. E. L. Clarke,⁵⁸ M. Clemencic,⁴⁸ H. V. Cliff,⁵⁵ J. Closier,⁴⁸ J. L. Cobbledick,⁶² V. Coco,⁴⁸ J. A. B. Coelho,¹¹ J. Cogan,¹⁰ E. Cogneras,⁹ L. Cojocariu,³⁷ P. Collins,⁴⁸ T. Colombo,⁴⁸ L. Congedo,^{19,g} A. Contu,²⁷ N. Cooke,⁵³ G. Coombs,⁵⁹ I. Corredoira,⁴⁶ G. Corti,⁴⁸ C. M. Costa Sobral,⁵⁶ B. Couturier,⁴⁸ D. C. Craik,⁶⁴ J. Crkovská,⁶⁷ M. Cruz Torres,¹ R. Currie,⁵⁸ C. L. Da Silva,⁶⁷ S. Dadabaev,⁸³ L. Dai,⁷¹ E. Dall'Occo,¹⁵ J. Dalseno,⁴⁶ C. D'Ambrosio,⁴⁸ A. Danilina,⁴¹ P. d'Argent,⁴⁸ J. E. Davies,⁶² A. Davis,⁶² O. De Aguiar Francisco,⁶² K. De Bruyn,⁷⁹ S. De Capua,⁶² M. De Cian,⁴⁹ J. M. De Miranda,¹ L. De Paula,² M. De Serio,^{19,g} D. De Simone,⁵⁰ P. De Simone,²³ F. De Vellis,¹⁵ J. A. de Vries,⁸⁰ C. T. Dean,⁶⁷ F. Debernardis,^{19,g} D. Decamp,⁸ V. Dedu,¹⁰ L. Del Buono,¹³ B. Delaney,⁵⁵ H.-P. Dembinski,¹⁵ A. Dendek,³⁴ V. Denysenko,⁵⁰ D. Derkach,⁸² O. Deschamps,⁹ F. Desse,¹¹ F. Dettori,^{27,h} B. Dey,⁷⁷ A. Di Cicco,²³ P. Di Nezza,²³ S. Didenko,⁸³ L. Dieste Maronas,⁴⁶ H. Dijkstra,⁴⁸ V. Dobishuk,⁵² C. Dong,³ A. M. Donohoe,¹⁸ F. Dordei,²⁷ A. C. dos Reis,¹ L. Douglas,⁵⁹ A. Dovbnja,⁵¹ A. G. Downes,⁸ M. W. Dudek,³⁵ L. Dufour,⁴⁸ V. Duk,⁷⁸ P. Durante,⁴⁸ J. M. Durham,⁶⁷ D. Dutta,⁶² A. Dziurda,³⁵ A. Dzyuba,³⁸ S. Easo,⁵⁷ U. Egede,⁶⁹ V. Egorychev,⁴¹ S. Eidelman,^{43,a,i} S. Eisenhardt,⁵⁸ S. Ek-In,⁴⁹ L. Eklund,^{59,86} S. Ely,⁶⁸ A. Ene,³⁷ E. Epple,⁶⁷ S. Escher,¹⁴ J. Eschle,⁵⁰ S. Esen,¹³ T. Evans,⁴⁸ A. Falabella,²⁰ J. Fan,³ Y. Fan,⁶ B. Fang,⁷³ S. Farry,⁶⁰ D. Fazzini,^{26,e} M. Féo,⁴⁸ A. Fernandez Prieto,⁴⁶ A. D. Fernez,⁶⁶ F. Ferrari,^{20,f} L. Ferreira Lopes,⁴⁹ F. Ferreira Rodrigues,² S. Ferreres Sole,³² M. Ferrillo,⁵⁰ M. Ferro-Luzzi,⁴⁸ S. Filippov,³⁹ R. A. Fini,¹⁹ M. Fiorini,^{21,d} M. Firlej,³⁴ K. M. Fischer,⁶³ D. S. Fitzgerald,⁸⁷ C. Fitzpatrick,⁶² T. Fiutowski,³⁴ A. Fkiaras,⁴⁸ F. Fleuret,¹² M. Fontana,¹³ F. Fontanelli,^{24,b} R. Forty,⁴⁸ D. Foulds-Holt,⁵⁵ V. Franco Lima,⁶⁰ M. Franco Sevilla,⁶⁶ M. Frank,⁴⁸ E. Franzoso,²¹ G. Frau,¹⁷ C. Frei,⁴⁸ D. A. Friday,⁵⁹ J. Fu,⁶ Q. Fuehring,¹⁵ E. Gabriel,³² G. Galati,^{19,g} A. Gallas Torreira,⁴⁶ D. Galli,^{20,f} S. Gambetta,^{58,48} Y. Gan,³ M. Gandelman,² P. Gandini,²⁵ Y. Gao,⁵ M. Garau,²⁷ L. M. Garcia Martin,⁵⁶ P. Garcia Moreno,⁴⁵ J. García Pardiñas,^{26,e} B. Garcia Plana,⁴⁶ F. A. Garcia Rosales,¹² L. Garrido,⁴⁵ C. Gaspar,⁴⁸ R. E. Geertsema,³² D. Gerick,¹⁷ L. L. Gerken,¹⁵ E. Gersabeck,⁶² M. Gersabeck,⁶² T. Gershon,⁵⁶ D. Gerstel,¹⁰ L. Giambastiani,²⁸ V. Gibson,⁵⁵ H. K. Giemza,³⁶ A. L. Gilman,⁶³ M. Giovannetti,^{23,j} A. Gioventù,⁴⁶ P. Gironella Gironell,⁴⁵ L. Giubega,³⁷ C. Giugliano,^{21,48,d} K. Gizzdov,⁵⁸ E. L. Gkougkousis,⁴⁸ V. V. Gligorov,¹³ C. Göbel,⁷⁰ E. Golobardes,⁸⁵ D. Golubkov,⁴¹ A. Golutvin,^{61,83} A. Gomes,^{1,k} S. Gomez Fernandez,⁴⁵ F. Goncalves Abrantes,⁶³ M. Goncerz,³⁵ G. Gong,³ P. Gorbovov,⁴¹ I. V. Gorelov,⁴⁰ C. Gotti,²⁶ E. Govorkova,⁴⁸ J. P. Grabowski,¹⁷ T. Grammatico,¹³ L. A. Granado Cardoso,⁴⁸ E. Graugés,⁴⁵ E. Graverini,⁴⁹ G. Graziani,²² A. Grecu,³⁷ L. M. Greeven,³² N. A. Grieser,⁴ L. Grillo,⁶² S. Gromov,⁸³ B. R. Gruberg Cazon,⁶³ C. Gu,³ M. Guarise,²¹ M. Guittiere,¹¹ P. A. Günther,¹⁷ E. Gushchin,³⁹ A. Guth,¹⁴ Y. Guz,⁴⁴ T. Gys,⁴⁸ T. Hadavizadeh,⁶⁹ G. Haefeli,⁴⁹ C. Haen,⁴⁸ J. Haimberger,⁴⁸ T. Halewood-leagases,⁶⁰ P. M. Hamilton,⁶⁶ J. P. Hammerich,⁶⁰ Q. Han,⁷ X. Han,¹⁷ T. H. Hancock,⁶³

- E. B. Hansen,⁶² S. Hansmann-Menzemer,¹⁷ N. Harnew,⁶³ T. Harrison,⁶⁰ C. Hasse,⁴⁸ M. Hatch,⁴⁸ J. He,^{6,1} M. Hecker,⁶¹ K. Heijhoff,³² K. Heinicke,¹⁵ A. M. Hennequin,⁴⁸ K. Hennessy,⁶⁰ L. Henry,⁴⁸ J. Heuel,¹⁴ A. Hicheur,² D. Hill,⁴⁹ M. Hilton,⁶² S. E. Hollitt,¹⁵ R. Hou,⁷ Y. Hou,⁸ J. Hu,¹⁷ J. Hu,⁷² W. Hu,⁷ X. Hu,³ W. Huang,⁶ X. Huang,⁷³ W. Hulsbergen,³² R. J. Hunter,⁵⁶ M. Hushchyn,⁸² D. Hutchcroft,⁶⁰ D. Hynds,³² P. Ibis,¹⁵ M. Idzik,³⁴ D. Ilin,³⁸ P. Ilten,⁶⁵ A. Inglessi,³⁸ A. Ishteev,⁸³ K. Ivshin,³⁸ R. Jacobsson,⁴⁸ H. Jage,¹⁴ S. Jakobsen,⁴⁸ E. Jans,³² B. K. Jashal,⁴⁷ A. Jawahery,⁶⁶ V. Jevtic,¹⁵ F. Jiang,³ M. John,⁶³ D. Johnson,⁴⁸ C. R. Jones,⁵⁵ T. P. Jones,⁵⁶ B. Jost,⁴⁸ N. Jurik,⁴⁸ S. H. Kalavan Kadavath,³⁴ S. Kandybei,⁵¹ Y. Kang,³ M. Karacson,⁴⁸ M. Karpov,⁸² F. Keizer,⁴⁸ D. M. Keller,⁶⁸ M. Kenzie,⁵⁶ T. Ketel,³³ B. Khanji,¹⁵ A. Kharisova,⁸⁴ S. Kholodenko,⁴⁴ T. Kirn,¹⁴ V. S. Kirsebom,⁴⁹ O. Kitouni,⁶⁴ S. Klaver,³² N. Kleijne,²⁹ K. Klimaszewski,³⁶ M. R. Kmiec,³⁶ S. Kolliiev,⁵² A. Kondybayeva,⁸³ A. Konoplyannikov,⁴¹ P. Kopciewicz,³⁴ R. Kopecna,¹⁷ P. Koppenburg,³² M. Korolev,⁴⁰ I. Kostiuk,^{32,52} O. Kot,⁵² S. Kotriakhova,^{21,38} P. Kravchenko,³⁸ L. Kravchuk,³⁹ R. D. Krawczyk,⁴⁸ M. Kreps,⁵⁶ F. Kress,⁶¹ S. Kretzschmar,¹⁴ P. Krokovny,^{43,i} W. Krupa,³⁴ W. Krzemien,³⁶ M. Kucharczyk,³⁵ V. Kudryavtsev,^{43,i} H. S. Kuindersma,^{32,33} G. J. Kunde,⁶⁷ T. Kvaratskheliya,⁴¹ D. Lacarrere,⁴⁸ G. Lafferty,⁶² A. Lai,²⁷ A. Lampis,²⁷ D. Lancierini,⁵⁰ J. J. Lane,⁶² R. Lane,⁵⁴ G. Lanfranchi,²³ C. Langenbruch,¹⁴ J. Langer,¹⁵ O. Lantwin,⁸³ T. Latham,⁵⁶ F. Lazzari,^{29,m} R. Le Gac,¹⁰ S. H. Lee,⁸⁷ R. Lefèvre,⁹ A. Leflat,⁴⁰ S. Legotin,⁸³ O. Leroy,¹⁰ T. Lesiak,³⁵ B. Leverington,¹⁷ H. Li,⁷² P. Li,¹⁷ S. Li,⁷ Y. Li,⁴ Y. Li,⁴ Z. Li,⁶⁸ X. Liang,⁶⁸ T. Lin,⁶¹ R. Lindner,⁴⁸ V. Lisovskyi,¹⁵ R. Litvinov,²⁷ G. Liu,⁷² H. Liu,⁶ Q. Liu,⁶ S. Liu,⁴ A. Lobo Salvia,⁴⁵ A. Loi,²⁷ J. Lomba Castro,⁴⁶ I. Longstaff,⁵⁹ J. H. Lopes,² S. Lopez Solino,⁴⁶ G. H. Lovell,⁵⁵ Y. Lu,⁴ C. Lucarelli,²² D. Lucchesi,^{28,n} S. Luchuk,³⁹ M. Lucio Martinez,³² V. Lukashenko,^{32,52} Y. Luo,³ A. Lupato,⁶² E. Luppi,^{21,d} O. Lupton,⁵⁶ A. Lusiani,^{29,o} X. Lyu,⁶ L. Ma,⁴ R. Ma,⁶ S. Maccolini,^{20,f} F. Machefert,¹¹ F. Maciuc,³⁷ V. Macko,⁴⁹ P. Mackowiak,¹⁵ S. Maddrell-Mander,⁵⁴ O. Madejczyk,³⁴ L. R. Madhan Mohan,⁵⁴ O. Maev,³⁸ A. Maevskiy,⁸² D. Maisuzenko,³⁸ M. W. Majewski,³⁴ J. J. Malczewski,³⁵ S. Malde,⁶³ B. Malecki,⁴⁸ A. Malinin,⁸¹ T. Maltsev,^{43,i} H. Malygina,¹⁷ G. Manca,^{27,h} G. Mancinelli,¹⁰ D. Manuzzi,^{20,f} D. Marangotto,^{25,p} J. Maratas,^{9,q} J. F. Marchand,⁸ U. Marconi,²⁰ S. Mariani,^{22,r} C. Marin Benito,⁴⁸ M. Marinangeli,⁴⁹ J. Marks,¹⁷ A. M. Marshall,⁵⁴ P. J. Marshall,⁶⁰ G. Martelli,⁷⁸ G. Martellotti,³⁰ L. Martinazzoli,^{48,e} M. Martinelli,^{26,e} D. Martinez Santos,⁴⁶ F. Martinez Vidal,⁴⁷ A. Massafferri,¹ M. Materok,¹⁴ R. Matev,⁴⁸ A. Mathad,⁵⁰ V. Matiunin,⁴¹ C. Matteuzzi,²⁶ K. R. Mattioli,⁸⁷ A. Mauri,³² E. Maurice,¹² J. Mauricio,⁴⁵ M. Mazurek,⁴⁸ M. McCann,⁶¹ L. McConnell,¹⁸ T. H. McGrath,⁶² N. T. Mchugh,⁵⁹ A. McNab,⁶² R. McNulty,¹⁸ J. V. Mead,⁶⁰ B. Meadows,⁶⁵ G. Meier,¹⁵ N. Meinert,⁷⁶ D. Melnychuk,³⁶ S. Meloni,^{26,e} M. Merk,^{32,80} A. Merli,^{25,p} L. Meyer Garcia,² M. Mikhasenko,⁴⁸ D. A. Milanes,⁷⁴ E. Millard,⁵⁶ M. Milovanovic,⁴⁸ M.-N. Minard,⁸ A. Minotti,^{26,e} L. Minzoni,^{21,d} S. E. Mitchell,⁵⁸ B. Mitreska,⁶² D. S. Mitzel,¹⁵ A. Mödden,¹⁵ R. A. Mohammed,⁶³ R. D. Moise,⁶¹ S. Mokhnenko,⁸² T. Mombächer,⁴⁶ I. A. Monroy,⁷⁴ S. Monteil,⁹ M. Morandin,²⁸ G. Morello,²³ M. J. Morello,^{29,o} J. Moron,³⁴ A. B. Morris,⁷⁵ A. G. Morris,⁵⁶ R. Mountain,⁶⁸ H. Mu,³ F. Muheim,^{58,48} M. Mulder,⁴⁸ D. Müller,⁴⁸ K. Müller,⁵⁰ C. H. Murphy,⁶³ D. Murray,⁶² P. Muzzetto,^{27,48} P. Naik,⁵⁴ T. Nakada,⁴⁹ R. Nandakumar,⁵⁷ T. Nanut,⁴⁹ I. Nasteva,² M. Needham,⁵⁸ I. Neri,²¹ N. Neri,^{25,p} S. Neubert,⁷⁵ N. Neufeld,⁴⁸ R. Newcombe,⁶¹ E. M. Niel,¹¹ S. Nieswand,¹⁴ N. Nikitin,⁴⁰ N. S. Nolte,⁶⁴ C. Normand,⁸ C. Nunez,⁸⁷ A. Oblakowska-Mucha,³⁴ V. Obraztsov,⁴⁴ T. Oeser,¹⁴ D. P. O'Hanlon,⁵⁴ S. Okamura,²¹ R. Oldeman,^{27,h} F. Oliva,⁵⁸ M. E. Olivares,⁶⁸ C. J. G. Onderwater,⁷⁹ R. H. O'Neil,⁵⁸ J. M. Otalora Goicochea,² T. Ovsiannikova,⁴¹ P. Owen,⁵⁰ A. Oyanguren,⁴⁷ K. O. Padeken,⁷⁵ B. Pagare,⁵⁶ P. R. Pais,⁴⁸ T. Pajero,⁶³ A. Palano,¹⁹ M. Palutan,²³ Y. Pan,⁶² G. Panshin,⁸⁴ A. Papanestis,⁵⁷ M. Pappagallop,^{19,g} L. L. Pappalardo,^{21,d} C. Pappenheimer,⁶⁵ W. Parker,⁶⁶ C. Parkes,⁶² B. Passalacqua,²¹ G. Passaleva,²² A. Pastore,¹⁹ M. Patel,⁶¹ C. Patrignani,^{20,f} C. J. Pawley,⁸⁰ A. Pearce,⁴⁸ A. Pellegrino,³² M. Pepe Altarelli,⁴⁸ S. Perazzini,²⁰ D. Pereira,⁴¹ A. Pereiro Castro,⁴⁶ P. Perret,⁹ M. Petric,^{59,48} K. Petridis,⁵⁴ A. Petrolini,^{24,b} A. Petrov,⁸¹ S. Petrucci,⁵⁸ M. Petruzzo,²⁵ T. T. H. Pham,⁶⁸ A. Philippov,⁴² L. Pica,^{29,o} M. Piccini,⁷⁸ B. Pietrzyk,⁸ G. Pietrzyk,⁴⁹ M. Pili,⁶³ D. Pinci,³⁰ F. Pisani,⁴⁸ M. Pizzichemi,^{26,48,e} Resmi P. K.,¹⁰ V. Placinta,³⁷ J. Plews,⁵³ M. Plo Casasus,⁴⁶ F. Polci,¹³ M. Poli Lener,²³ M. Poliakova,⁶⁸ A. Poluektov,¹⁰ N. Polukhina,^{83,s} I. Polyakov,⁶⁸ E. Polycarpo,² S. Ponce,⁴⁸ D. Popov,^{6,48} S. Popov,⁴² S. Poslavskii,⁴⁴ K. Prasanth,³⁵ L. Promberger,⁴⁸ C. Prouve,⁴⁶ V. Pugatch,⁵² V. Puill,¹¹ H. Pullen,⁶³ G. Punzi,^{29,t} H. Qi,³ W. Qian,⁶ J. Qin,⁶ N. Qin,³ R. Quagliani,⁴⁹ B. Quintana,⁸ N. V. Raab,¹⁸ R. I. Rabidan Trejo,⁶ B. Rachwal,³⁴ J. H. Rademacker,⁵⁴ M. Rama,²⁹ M. Ramos Pernas,⁵⁶ M. S. Rangel,² F. Ratnikov,^{42,82} G. Raven,³³ M. Reboud,⁸ F. Redi,⁴⁹ F. Reiss,⁶² C. Remon Alepuz,⁴⁷ Z. Ren,³ V. Renaudin,⁶³ R. Ribatti,²⁹ S. Ricciardi,⁵⁷ K. Rinnert,⁶⁰ P. Robbe,¹¹ G. Robertson,⁵⁸ A. B. Rodrigues,⁴⁹ E. Rodrigues,⁶⁰ J. A. Rodriguez Lopez,⁷⁴ E. R. R. Rodriguez Rodriguez,⁴⁶ A. Rollings,⁶³ P. Roloff,⁴⁸ V. Romanovskiy,⁴⁴ M. Romero Lamas,⁴⁶ A. Romero Vidal,⁴⁶ J. D. Roth,⁸⁷ M. Rotondo,²³ M. S. Rudolph,⁶⁸ T. Ruf,⁴⁸ R. A. Ruiz Fernandez,⁴⁶ J. Ruiz Vidal,⁴⁷ A. Ryzhikov,⁸² J. Ryzka,³⁴ J. J. Saborido Silva,⁴⁶ N. Sagidova,³⁸ N. Sahoo,⁵⁶ B. Saitta,^{27,h} M. Salomoni,⁴⁸

C. Sanchez Gras,³² R. Santacesaria,³⁰ C. Santamarina Rios,⁴⁶ M. Santimaria,²³ E. Santovetti,^{31,j} D. Saranin,⁸³ G. Sarpis,¹⁴ M. Sarpis,⁷⁵ A. Sarti,³⁰ C. Satriano,^{30,u} A. Satta,³¹ M. Saur,¹⁵ D. Savrina,^{41,40} H. Sazak,⁹ L. G. Scantlebury Smead,⁶³ A. Scarabotto,¹³ S. Schael,¹⁴ S. Scherl,⁶⁰ M. Schiller,⁵⁹ H. Schindler,⁴⁸ M. Schmelling,¹⁶ B. Schmidt,⁴⁸ S. Schmitt,¹⁴ O. Schneider,⁴⁹ A. Schopper,⁴⁸ M. Schubiger,³² S. Schulte,⁴⁹ M. H. Schune,¹¹ R. Schwemmer,⁴⁸ B. Sciascia,^{23,48} S. Sellam,⁴⁶ A. Semennikov,⁴¹ M. Senghi Soares,³³ A. Sergi,^{24,b} N. Serra,⁵⁰ L. Sestini,²⁸ A. Seuthe,¹⁵ Y. Shang,⁵ D. M. Shangase,⁸⁷ M. Shapkin,⁴⁴ I. Shchemberov,⁸³ L. Shchutska,⁴⁹ T. Shears,⁶⁰ L. Shekhtman,^{43,i} Z. Shen,⁵ V. Shevchenko,⁸¹ E. B. Shields,^{26,e} Y. Shimizu,¹¹ E. Shmanin,⁸³ J. D. Shupperd,⁶⁸ B. G. Siddi,²¹ R. Silva Coutinho,⁵⁰ G. Simi,²⁸ S. Simone,^{19,g} N. Skidmore,⁶² T. Skwarnicki,⁶⁸ M. W. Slater,⁵³ I. Slazyk,^{21,d} J. C. Smallwood,⁶³ J. G. Smeaton,⁵⁵ A. Smetkina,⁴¹ E. Smith,⁵⁰ M. Smith,⁶¹ A. Snoch,³² M. Soares,²⁰ L. Soares Lavra,⁹ M. D. Sokoloff,⁶⁵ F. J. P. Soler,⁵⁹ A. Solovev,³⁸ I. Solovyev,³⁸ F. L. Souza De Almeida,² B. Souza De Paula,² B. Spaan,¹⁵ E. Spadaro Norella,^{25,p} P. Spradlin,⁵⁹ F. Stagni,⁴⁸ M. Stahl,⁶⁵ S. Stahl,⁴⁸ S. Stanislaus,⁶³ O. Steinkamp,^{50,83} O. Stenyakin,⁴⁴ H. Stevens,¹⁵ S. Stone,⁶⁸ M. Straticiuc,³⁷ D. Strekalina,⁸³ F. Suljik,⁶³ J. Sun,²⁷ L. Sun,⁷³ Y. Sun,⁶⁶ P. Svhira,⁶² P. N. Swallow,⁵³ K. Swientek,³⁴ A. Szabelski,³⁶ T. Szumlak,³⁴ M. Szymanski,⁴⁸ S. Taneja,⁶² A. R. Tanner,⁵⁴ M. D. Tat,⁶³ A. Terentev,⁸³ F. Teubert,⁴⁸ E. Thomas,⁴⁸ D. J. D. Thompson,⁵³ K. A. Thomson,⁶⁰ V. Tisserand,⁹ S. T'Jampens,⁸ M. Tobin,⁴ L. Tomassetti,^{21,d} X. Tong,⁵ D. Torres Machado,¹ D. Y. Tou,¹³ E. Trifonova,⁸³ C. Tripli,⁴⁹ G. Tuci,⁶ A. Tully,⁴⁹ N. Tuning,^{32,48} A. Ukleja,³⁶ D. J. Unverzagt,¹⁷ E. Ursov,⁸³ A. Usachov,³² A. Ustyuzhanin,^{42,82} U. Uwer,¹⁷ A. Vagner,⁸⁴ V. Vagnoni,²⁰ A. Valassi,⁴⁸ G. Valenti,²⁰ N. Valls Canudas,⁸⁵ M. van Beuzekom,³² M. Van Dijk,⁴⁹ H. Van Hecke,⁶⁷ E. van Herwijnen,⁸³ C. B. Van Hulse,¹⁸ M. van Veghel,⁷⁹ R. Vazquez Gomez,⁴⁵ P. Vazquez Regueiro,⁴⁶ C. Vázquez Sierra,⁴⁸ S. Vecchi,²¹ J. J. Velthuis,⁵⁴ M. Veltri,^{22,v} A. Venkateswaran,⁶⁸ M. Veronesi,³² M. Vesterinen,⁵⁶ D. Vieira,⁶⁵ M. Vieites Diaz,⁴⁹ H. Viemann,⁷⁶ X. Vilasis-Cardona,⁸⁵ E. Vilella Figueras,⁶⁰ A. Villa,²⁰ P. Vincent,¹³ F. C. Volle,¹¹ D. Vom Bruch,¹⁰ A. Vorobyev,³⁸ V. Vorobyev,^{43,i} N. Voropaev,³⁸ K. Vos,⁸⁰ R. Waldi,¹⁷ J. Walsh,²⁹ C. Wang,¹⁷ J. Wang,⁵ J. Wang,⁴ J. Wang,³ J. Wang,⁷³ M. Wang,³ R. Wang,⁵⁴ Y. Wang,⁷ Z. Wang,⁵⁰ Z. Wang,³ Z. Wang,⁶ J. A. Ward,⁵⁶ N. K. Watson,⁵³ S. G. Weber,¹³ D. Websdale,⁶¹ C. Weisser,⁶⁴ B. D. C. Westhenry,⁵⁴ D. J. White,⁶² M. Whitehead,⁵⁴ A. R. Wiederhold,⁵⁶ D. Wiedner,¹⁵ G. Wilkinson,⁶³ M. Wilkinson,⁶⁸ I. Williams,⁵⁵ M. Williams,⁶⁴ M. R. J. Williams,⁵⁸ F. F. Wilson,⁵⁷ W. Wislicki,³⁶ M. Witek,³⁵ L. Witola,¹⁷ G. Wormser,¹¹ S. A. Wotton,⁵⁵ H. Wu,⁶⁸ K. Wyllie,⁴⁸ Z. Xiang,⁶ D. Xiao,⁷ Y. Xie,⁷ A. Xu,⁵ J. Xu,⁶ L. Xu,³ M. Xu,⁷ Q. Xu,⁶ Z. Xu,⁵ Z. Xu,⁶ D. Yang,³ S. Yang,⁶ Y. Yang,⁶ Z. Yang,⁵ Z. Yang,⁶⁶ Y. Yao,⁶⁸ L. E. Yeomans,⁶⁰ H. Yin,⁷ J. Yu,⁷¹ X. Yuan,⁶⁸ O. Yushchenko,⁴⁴ E. Zaffaroni,⁴⁹ M. Zavertyaev,^{16,s} M. Zdybal,³⁵ O. Zenaiev,⁴⁸ M. Zeng,³ D. Zhang,⁷ L. Zhang,³ S. Zhang,⁷¹ S. Zhang,⁵ Y. Zhang,⁶³ A. Zharkova,⁸³ A. Zhelezov,¹⁷ Y. Zheng,⁶ T. Zhou,⁵ X. Zhou,⁶ Y. Zhou,⁶ V. Zhovkovska,¹¹ X. Zhu,³ X. Zhu,⁷ Z. Zhu,⁶ V. Zhukov,^{14,40} J. B. Zonneveld,⁵⁸ Q. Zou,⁴ S. Zucchelli,^{20,f} D. Zuliani,²⁸ and G. Zunica⁶²

(LHCb Collaboration)

¹Centro Brasileiro de Pesquisas Físicas (CBPF), Rio de Janeiro, Brazil²Universidade Federal do Rio de Janeiro (UFRJ), Rio de Janeiro, Brazil³Center for High Energy Physics, Tsinghua University, Beijing, China⁴Institute Of High Energy Physics (IHEP), Beijing, China⁵School of Physics State Key Laboratory of Nuclear Physics and Technology, Peking University, Beijing, China⁶University of Chinese Academy of Sciences, Beijing, China⁷Institute of Particle Physics, Central China Normal University, Wuhan, Hubei, China⁸Université Savoie Mont Blanc, CNRS, IN2P3-LAPP, Annecy, France⁹Université Clermont Auvergne, CNRS/IN2P3, LPC, Clermont-Ferrand, France¹⁰Aix Marseille Univ, CNRS/IN2P3, CPPM, Marseille, France¹¹Université Paris-Saclay, CNRS/IN2P3, IJCLab, Orsay, France¹²Laboratoire Leprince-Ringuet, CNRS/IN2P3, Ecole Polytechnique, Institut Polytechnique de Paris, Palaiseau, France¹³LPNHE, Sorbonne Université, Paris Diderot Sorbonne Paris Cité, CNRS/IN2P3, Paris, France¹⁴I. Physikalisches Institut, RWTH Aachen University, Aachen, Germany¹⁵Fakultät Physik, Technische Universität Dortmund, Dortmund, Germany¹⁶Max-Planck-Institut für Kernphysik (MPIK), Heidelberg, Germany¹⁷Physikalischs Institut, Ruprecht-Karls-Universität Heidelberg, Heidelberg, Germany¹⁸School of Physics, University College Dublin, Dublin, Ireland¹⁹INFN Sezione di Bari, Bari, Italy

- ²⁰INFN Sezione di Bologna, Bologna, Italy
²¹INFN Sezione di Ferrara, Ferrara, Italy
²²INFN Sezione di Firenze, Firenze, Italy
²³INFN Laboratori Nazionali di Frascati, Frascati, Italy
²⁴INFN Sezione di Genova, Genova, Italy
²⁵INFN Sezione di Milano, Milano, Italy
²⁶INFN Sezione di Milano-Bicocca, Milano, Italy
²⁷INFN Sezione di Cagliari, Monserrato, Italy
²⁸Università degli Studi di Padova, Università e INFN, Padova, Padova, Italy
²⁹INFN Sezione di Pisa, Pisa, Italy
³⁰INFN Sezione di Roma La Sapienza, Roma, Italy
³¹INFN Sezione di Roma Tor Vergata, Roma, Italy
³²Nikhef National Institute for Subatomic Physics, Amsterdam, Netherlands
³³Nikhef National Institute for Subatomic Physics and VU University Amsterdam, Amsterdam, Netherlands
³⁴AGH—University of Science and Technology, Faculty of Physics and Applied Computer Science, Kraków, Poland
³⁵Henryk Niewodniczanski Institute of Nuclear Physics Polish Academy of Sciences, Kraków, Poland
³⁶National Center for Nuclear Research (NCBJ), Warsaw, Poland
³⁷Horia Hulubei National Institute of Physics and Nuclear Engineering, Bucharest-Magurele, Romania
³⁸Petersburg Nuclear Physics Institute NRC Kurchatov Institute (PNPI NRC KI), Gatchina, Russia
³⁹Institute for Nuclear Research of the Russian Academy of Sciences (INR RAS), Moscow, Russia
⁴⁰Institute of Nuclear Physics, Moscow State University (SINP MSU), Moscow, Russia
⁴¹Institute of Theoretical and Experimental Physics NRC Kurchatov Institute (ITEP NRC KI), Moscow, Russia
⁴²Yandex School of Data Analysis, Moscow, Russia
⁴³Budker Institute of Nuclear Physics (SB RAS), Novosibirsk, Russia
⁴⁴Institute for High Energy Physics NRC Kurchatov Institute (IHEP NRC KI), Protvino, Russia, Protvino, Russia
⁴⁵ICCUB, Universitat de Barcelona, Barcelona, Spain
⁴⁶Instituto Galego de Física de Altas Enerxías (IGFAE), Universidade de Santiago de Compostela, Santiago de Compostela, Spain
⁴⁷Instituto de Fisica Corpuscular, Centro Mixto Universidad de Valencia—CSIC, Valencia, Spain
⁴⁸European Organization for Nuclear Research (CERN), Geneva, Switzerland
⁴⁹Institute of Physics, Ecole Polytechnique Fédérale de Lausanne (EPFL), Lausanne, Switzerland
⁵⁰Physik-Institut, Universität Zürich, Zürich, Switzerland
⁵¹NSC Kharkiv Institute of Physics and Technology (NSC KIPT), Kharkiv, Ukraine
⁵²Institute for Nuclear Research of the National Academy of Sciences (KINR), Kyiv, Ukraine
⁵³University of Birmingham, Birmingham, United Kingdom
⁵⁴H.H. Wills Physics Laboratory, University of Bristol, Bristol, United Kingdom
⁵⁵Cavendish Laboratory, University of Cambridge, Cambridge, United Kingdom
⁵⁶Department of Physics, University of Warwick, Coventry, United Kingdom
⁵⁷STFC Rutherford Appleton Laboratory, Didcot, United Kingdom
⁵⁸School of Physics and Astronomy, University of Edinburgh, Edinburgh, United Kingdom
⁵⁹School of Physics and Astronomy, University of Glasgow, Glasgow, United Kingdom
⁶⁰Oliver Lodge Laboratory, University of Liverpool, Liverpool, United Kingdom
⁶¹Imperial College London, London, United Kingdom
⁶²Department of Physics and Astronomy, University of Manchester, Manchester, United Kingdom
⁶³Department of Physics, University of Oxford, Oxford, United Kingdom
⁶⁴Massachusetts Institute of Technology, Cambridge, Massachusetts, United States
⁶⁵University of Cincinnati, Cincinnati, Ohio, United States
⁶⁶University of Maryland, College Park, Maryland, United States
⁶⁷Los Alamos National Laboratory (LANL), Los Alamos, New Mexico, United States
⁶⁸Syracuse University, Syracuse, New York, United States
⁶⁹School of Physics and Astronomy, Monash University, Melbourne, Australia
^(associated with Department of Physics, University of Warwick, Coventry, United Kingdom)
⁷⁰Pontifícia Universidade Católica do Rio de Janeiro (PUC-Rio), Rio de Janeiro, Brazil
^{(associated with Universidade Federal do Rio de Janeiro (UFRJ), Rio de Janeiro, Brazil)}
⁷¹Physics and Micro Electronic College, Hunan University, Changsha City, China
^(associated with Institute of Particle Physics, Central China Normal University, Wuhan, Hubei, China)
⁷²Guangdong Provincial Key Laboratory of Nuclear Science, Guangdong-Hong Kong Joint Laboratory of Quantum Matter, Institute of Quantum Matter, South China Normal University, Guangzhou, China
^(associated with Center for High Energy Physics, Tsinghua University, Beijing, China)

- ⁷³School of Physics and Technology, Wuhan University, Wuhan, China
 (associated with Center for High Energy Physics, Tsinghua University, Beijing, China)
- ⁷⁴Departamento de Fisica, Universidad Nacional de Colombia, Bogota, Colombia
 (associated with LPNHE, Sorbonne Université, Paris Diderot Sorbonne Paris Cité, CNRS/IN2P3, Paris, France)
- ⁷⁵Universität Bonn—Helmholtz-Institut für Strahlen und Kernphysik, Bonn, Germany
 (associated with Physikalisches Institut, Ruprecht-Karls-Universität Heidelberg, Heidelberg, Germany)
- ⁷⁶Institut für Physik, Universität Rostock, Rostock, Germany
 (associated with Physikalisches Institut, Ruprecht-Karls-Universität Heidelberg, Heidelberg, Germany)
- ⁷⁷Eotvos Lorand University, Budapest, Hungary
 (associated with European Organization for Nuclear Research (CERN), Geneva, Switzerland)
- ⁷⁸INFN Sezione di Perugia, Perugia, Italy
 (associated with INFN Sezione di Ferrara, Ferrara, Italy)
- ⁷⁹Van Swinderen Institute, University of Groningen, Groningen, Netherlands
 (associated with Nikhef National Institute for Subatomic Physics, Amsterdam, Netherlands)
- ⁸⁰Universiteit Maastricht, Maastricht, Netherlands
 (associated with Nikhef National Institute for Subatomic Physics, Amsterdam, Netherlands)
- ⁸¹National Research Centre Kurchatov Institute, Moscow, Russia
 (associated with Institute of Theoretical and Experimental Physics NRC Kurchatov Institute (ITEP NRC KI), Moscow, Russia)
- ⁸²National Research University Higher School of Economics, Moscow, Russia
 (associated with Yandex School of Data Analysis, Moscow, Russia)
- ⁸³National University of Science and Technology “MISIS”, Moscow, Russia
 (associated with Institute of Theoretical and Experimental Physics NRC Kurchatov Institute (ITEP NRC KI), Moscow, Russia)
- ⁸⁴National Research Tomsk Polytechnic University, Tomsk, Russia
 (associated with Institute of Theoretical and Experimental Physics NRC Kurchatov Institute (ITEP NRC KI), Moscow, Russia)
- ⁸⁵DS4DS, La Salle, Universitat Ramon Llull, Barcelona, Spain
 (associated with ICCUB, Universitat de Barcelona, Barcelona, Spain)
- ⁸⁶Department of Physics and Astronomy, Uppsala University, Uppsala, Sweden
 (associated with School of Physics and Astronomy, University of Glasgow, Glasgow, United Kingdom)
- ⁸⁷University of Michigan, Ann Arbor, Michigan, United States
 (associated with Syracuse University, Syracuse, New York, United States)

^aDeceased.^bAlso at Università di Genova, Genova, Italy.^cAlso at Università di Modena e Reggio Emilia, Modena, Italy.^dAlso at Università di Ferrara, Ferrara, Italy.^eAlso at Università di Milano Bicocca, Milano, Italy.^fAlso at Università di Bologna, Bologna, Italy.^gAlso at Università di Bari, Bari, Italy.^hAlso at Università di Cagliari, Cagliari, Italy.ⁱAlso at Novosibirsk State University, Novosibirsk, Russia.^jAlso at Università di Roma Tor Vergata, Roma, Italy.^kAlso at Universidade Federal do Triângulo Mineiro (UFTM), Uberaba-MG, Brazil.^lAlso at Hangzhou Institute for Advanced Study, UCAS, Hangzhou, China.^mAlso at Università di Siena, Siena, Italy.ⁿAlso at Università di Padova, Padova, Italy.^oAlso at Scuola Normale Superiore, Pisa, Italy.^pAlso at Università degli Studi di Milano, Milano, Italy.^qAlso at MSU—Iligan Institute of Technology (MSU-IIT), Iligan, Philippines.^rAlso at Università di Firenze, Firenze, Italy.^sAlso at P.N. Lebedev Physical Institute, Russian Academy of Science (LPI RAS), Moscow, Russia.^tAlso at Università di Pisa, Pisa, Italy.^uAlso at Università della Basilicata, Potenza, Italy.^vAlso at Università di Urbino, Urbino, Italy.